ORIGINAL ARTICLE

A C G publications

Org. Commun. 7:3 (2014) 85-97

organic communications

Synthesis and bioevaluation of some phenolic diarylpropanes as anti-cancer agents

Kshama Kundu, Mrityunjay Tyagi, Birija S. Patro, Subrata Chattopadhyay and Sandip K. Nayak*

Bio-Organic Division, Bhabha Atomic Research Centre, Mumbai 400 085, India

(Received January 27, 2014; Revised April 3, 2014; Accepted September 5, 2014)

Abstract: A convenient synthesis of six phenolic diarylpropanes has been formulated. A $CuBr_2$-catalyzed regioselective reaction was the key step for bromination of the arylpropanes. All the compounds showed good cytotoxicity to the human lung cancer A549 cell line. However, only one of these compounds induced apoptosis and a G1 cell cycle arrest by augmenting cellular ROS status. Introduction of bromo-substitution at the aryl groups increased the cytotoxicity significantly, but that was mainly due to necrosis.

Keywords: Anti-cancer activity; apoptosis; $CuBr_2$-induced bromination; reactive oxygen species.

1. Introduction

Arylpropanoids are the major family of 'polyphenols' and constitute a large part of our daily diet. These are found throughout the plant kingdom, and are produced in response to biotic or abiotic stresses. Using human cell cultures in vitro, and in vivo animal models, the phenylpropanoids have been shown to modulate molecular and cellular processes[1]. Hence there has been increasing interest in these compounds as anticancer, anti-virus, anti-inflammatory, and antibacterial agents as well as UV screens for cosmetic products. Some of these compounds are reported to reduce the doses of antibiotics and eliminate drug resistance[2]. Of particular interest is the cancer chemopreventive and anti-tumor-promoting effects of some phenylpropanoids[3, 4]. The combination of phenylpropanoids with 5-fluorouracil showed good anti-cancer property against human cervical cancer (HeLa) cell line[5]. Chalcones are one of the abundant natural phenylpropanoids displaying various pharmacological effects, and are potential leads for the new safer drugs[6]. Some natural chalcones showed cytotoxicity[7] against prostate cancer cells and inhibition to cathepsins that are emerging therapeutic targets for anticancer drug development[8].

Cancer is a major worldwide problem and the second leading cause of mortality in developed countries[9, 10]. Due to the toxicity and drug resistance, development of effective new cancer therapies is an important goal in medicinal chemistry[11, 12]. Incorporation of various substituents in the chalcone rings may offer better anti-cancer agents, devoid of the side effects. Organobromine compounds are isolated in large numbers from natural sources[13], and several of them show a wide range of pharmaceutical profile such as antibiotic activity[14], cytotoxicty and calcium channel activation property[15], and lipoxygenases inhibition[16]. However, reports about the effect of halogen incorporation in the chalcone B ring on the anti-neoplastic property are contradictory. For example, some B-ring

*Corresponding author: E-mail: sknayak@barc.gov.in; Tel: +91-22-25592410, Fax: +91-22-25505151

The article was published by Academy of Chemistry of Globe Publications
www.acgpubs.org/OC/index.htm © Published 9/30/2014 EISSN:1307-6175

bromo-substituted chalcones showed excellent cytotoxicity against the A549 cell line at very low concentrations (10^{-4} to 10^{-5} M)[17] while incorporation of a 4-fluoro, but not a 4-bromo group at chalcone B ring improved the topoisomerase I, and cathepsins B and L inhibitory activities[18]. On the other hand, the nature of the halogen (Br or F) substitution at C3 of the epipolythiodiketopiperazine alkaloids did not show any definite trend on their cytotoxicity [19].

Recently, isolation of three new **1**-**3** and one known **4** 1,3-diarylpropanes (Figure 1) from the MeOH extract of stems of the vine *Combretum griffithii* (Combretaceae) has been reported[20]. The aqueous decoction of the plant (known as "Khaminkhruea"[21] in Thai stems is traditionally used by local people for hepatitis treatment[22]. The 1,3-diarylpropanes **1**-**4** from *C. griffithii* stem extract were toxic to the KB oral human epidermal carcinoma cell line, with the relative potency as **3** >> **1** ~ **4** > extract >> **2**. Compound **3** was also cytotoxic against human NCI-H187 (IC_{50} = 1.08 μg/mL) and MCF7 (IC_{50} = 6.75 μg/mL) cancer cell lines. Compound **4** inhibited *Mycobacterium tuberculosis* (MIC 3.13 μg/mL), but none of these showed any activity against *Plasmodium falciparum*.

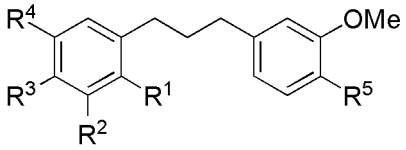

1 $R^1 = R^4 = OMe$, $R^2 = H$, $R^3 = R^5 = OH$
2 $R^1 = R^3 = OMe$, $R^2 = R^5 = OH$, $R^4 = H$
3 $R^1 = R^5 = OMe$, $R^2 = H$, $R^3 = R^4 = OH$
4 $R^1 = R^5 = OH$, $R^2 = R^4 = H$, $R^3 = OMe$

Figure 1. Chemical structure of the 1,3-diarypropanes from *C. griffithii* stem.

Identification of novel and selective anticancer agents remains an important and challenging goal in pharmacological research. In search of new compounds with strong antiproliferative activity and simple molecular structure, we synthesized six 1,3-diarylpropanes with different substitutions at the phenyl rings and evaluated their anti-cancer activity against the human non-small cell lung cancer (A549) cell line. Our primary aim was to examine the effect bromination on the proliferation of the A549 cells. To this end, the anti-cancer activity of two non-brominated **8a-b** and four brominated **9-12** diarylpropanes were compared. Given the importance of the phenolic moiety in anti-cancer property, we selected the compounds with phenolic groups at both the aromatic rings. Likewise, the compounds **9-12** possessed brominated aromatic rings. Further, the effect of some additional substitutions on the biological activity of the bromodiarylpropanes was also investigated.

2. Results and discussion

The initial motivation of the present work stems from our interest in natural and synthetic anti-neoplastic agents[23-28]. For the past several years, our group is interested synthesizing molecules containing the calixarene scaffold to study their ionophoric and host-guest inclusion properties for neutral molecules. In particular, exploration of the multifunctional spaces of bridged calixarenes and homocalixarenes are of special interest[29-32]. Many of these calixarene derivatives are easily amenable from suitably substituted diarylpropanes. Hence the selection of the target compounds was dictated in terms of their utility for the present studies as well as some homocalixarenes.

Chemistry: The synthesis (Scheme 1) commenced by the Aldol condensation of the acetophenones **5a** or **5b** with the aldehydes **6a** or **6b** respectively using ethanolic KOH as the base. This furnished the chalcones **7a** and **7b** in 73% and 75% yields respectively. Catalytic hydrogenation of the alkene function in **7a** and **7b** over 10% Pd-C in acetic acid directly afforded the diarylpropanes **8a** (84%) and **8b** (72%) via concomitant reduction of the benzylic ketone moiety. Recently, we have found that the combination of $CuBr_2/CH_3CN$ can brominate various phenolic compounds exclusively at the para-position[33]. Application of this protocol with **8a** produced the required dibromo compound **9** in almost quantitative yield. $MgCl_2$-catalyzed formylation of **9** led to the formation of a mixture of monoformyl **10** and diformyl **11** derivatives in ~2:3 ratio[34]. Reduction of **11** with $NaBH_4$ in MeOH proceeded uneventfully to furnish the dicarbinol **12** in 71% yield.

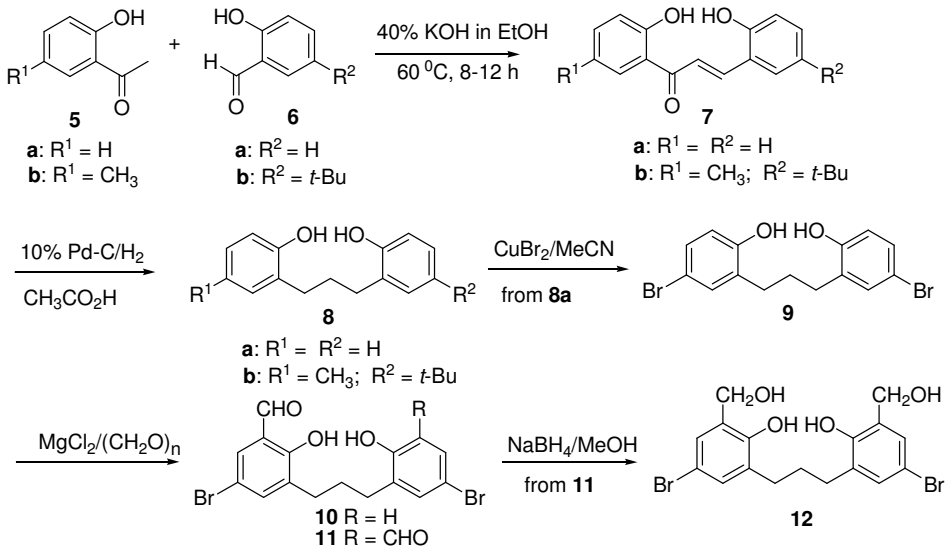

Scheme 1. Synthesis of phenolic diarylpropanes (**8-12**)

Biology: Lung cancer is the second leading cause of cancer-related deaths all over the world, with low survival rates in advanced stages[35, 36]. The poor prognosis is largely attributable to the inherent or acquired resistance in cancer cells against conventional chemotherapy. Hence, we examined the anti-proliferative potential of the diarylpropanes **8-12** against the highly invasive and metastatic human lung cancer A549 cells. Our MTT results at 48 h revealed that with respect to vehicle treated controls, all the compounds dose-dependently reduced viabilities of the A549 cells (Figure 2a). Based on a detailed dose-dependent MTT assay (Figure 2b) the growth inhibitory IC_{50} value of **8a** was found to be 66.1 ± 3.3 µM. Under identical conditions, the IC_{50} value of the positive control, curcumin was 29.1 ± 2.4 µM. The phase-contrast microscopy (Figure 3) showed that amongst

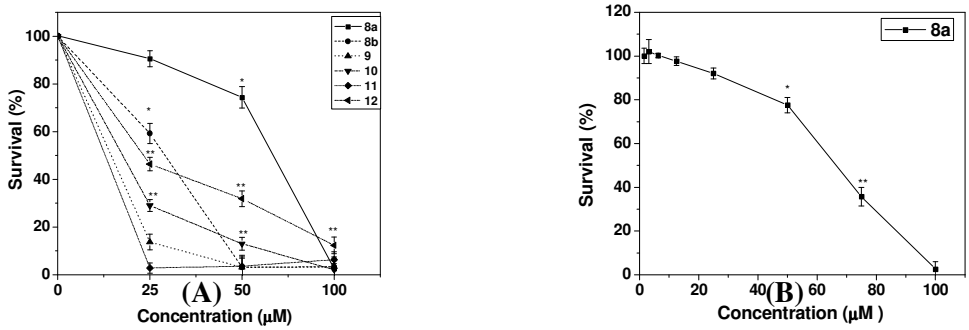

Figure 2. Dose-dependent cytotoxicity of the diarylpropanes **8a/b-12** against human lung carcinoma A549 cells. **(A)** Effect of compounds **8a/b-12**. **(B)** Effect of compound **8a** over a wide dose range. Cells (1 × 104/well), grown in 96-well plates were treated with vehicle (0.1% DMSO) or increasing concentrations of the test compounds. The cell viability was assessed by the MTT assay after 48 h. The results are expressed in percentage survival considering that of the vehicle-treated control cells as 100. The experiments were repeated three times with similar results. All determinations were made in four replicates, and the values are means ± S. E. M. *P<0.01, **P<0.001 compared to vehicle control.

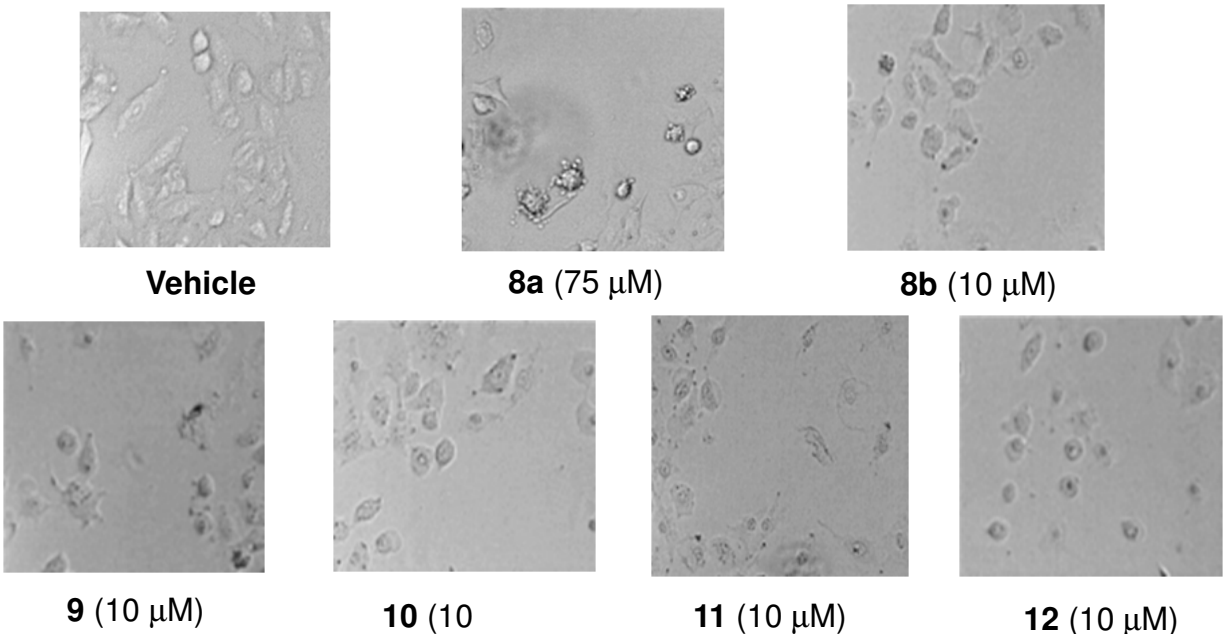

Figure 3. Alteration of A549 cells morphology as revealed by phase-contrast microscopy. The A549 cells (1×10^5 /well) in 6-well plates were treated with vehicle (0.1% DMSO) or the test compounds for 24 h, and visualized under a phase contrast microscope after washing with PBS. The experiments were repeated three times with similar results, and a representative image is shown.

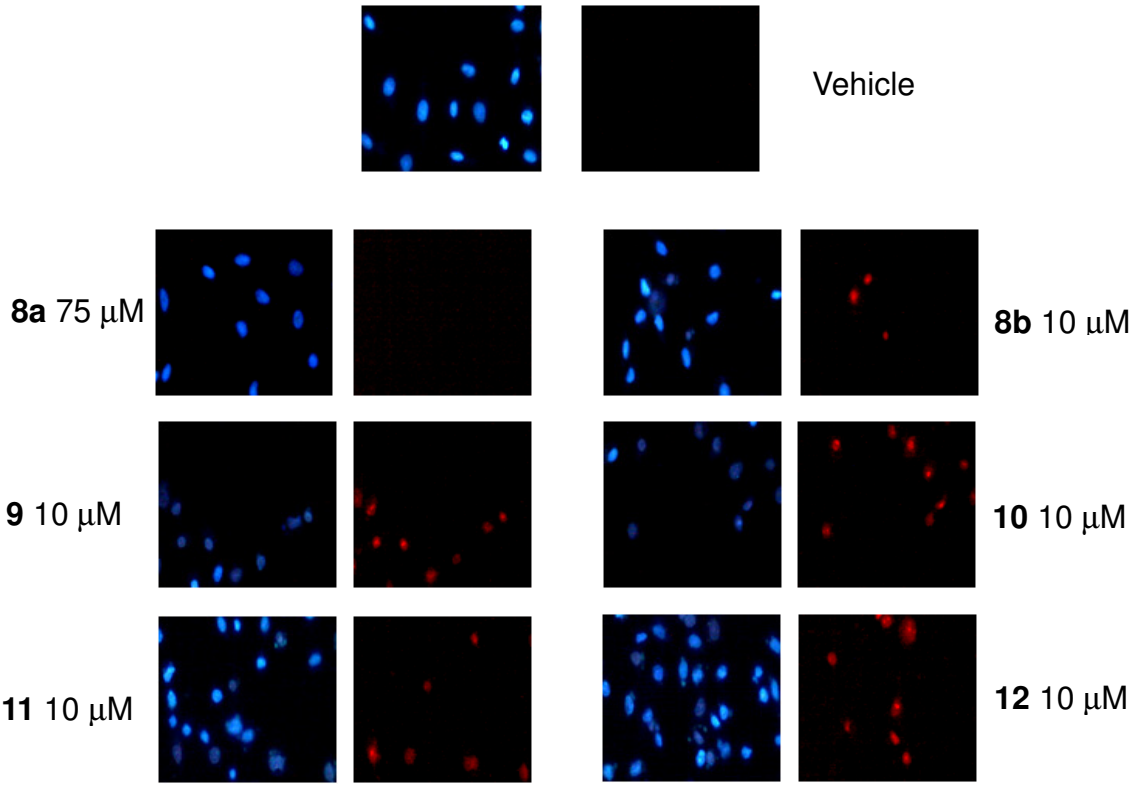

Figure 4. Detection of apoptosis/necrosis in the treated A549 cells by fluorescence microscopy. Cells were incubated with vehicle (0.1% DMSO) or the test compounds 3 h, stained with Hoechst 33342 and PI, and analyzed under Axioskop II Mot plus (Zeiss) microscope (40 × optics). The experiments were repeated three times with similar results, and a representative image is shown.

the test compounds only **8a** (75 µM) and to some extent **8b** (10 µM) induced significant morphological changes in the A549 cells, as the number of shrinking cells or those with blebbed membranes was notably increased after a 48 h. The other compounds induced necrosis, an undesirable mode of cell death. This was further confirmed by fluorescence microscopy after staining with Hoechst and propidium iodide (PI) (Figure 4). The nuclei of necrotic cells are characterized by red fluorescence on PI staining, while the nucleus of all the cells show blue fluorescence due to Hoechst staining. Our results showed significant necrosis at 3 h in the cells treated with the compounds **8b-12** even at a low concentration (10 µM). The phase-contrast and fluorescence microscopy results, obtained with higher concentrations of **8b-12** showed complete cell disruption (data not shown). Hence we did not determine the growth inhibitory IC_{50} values of **8b-12** despite the impressive MTT results (Figure 2a) that showed the relative potency of the test compounds as **11>9>10>12>8b>8a**. Since only **8a** did not induce any necrosis in the A549 cells, it was chosen for all subsequent studies.

Amongst the test samples, the 5/5' positions of **8b** are substituted with two different alkyl groups, while compounds **9-12** contain bromine substitutions in the aromatic ring/s. These will make them more lipophilic compared to compound **8a** that is devoid of any 5/5' substitution. As a result, compounds **8b** and **9-12** may predominantly accumulate at the cell membrane rather than at the mitochondria and/ or nucleus that is required for inducing apoptosis. Instead, these compounds may rupture the cell membrane, leading to necrosis.

Table 1. Dose-dependent effect of **8a** on A549 cell cycle

Phase	Cell population (%)				
	Vehicle	**8a** (µM)			
		25	50	75	100
% G1	57	62	67	80*	90*
% S	27	25	21	13*	6**
% G2	16	13	12	7*	4**

The values are mean of two independent experiments. *P<0.01, **P<0.001 compared to vehicle control.

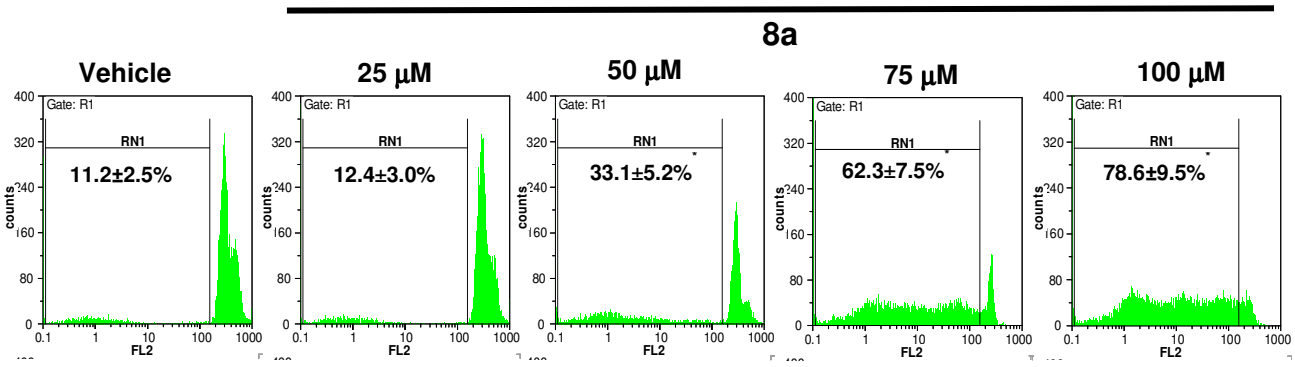

Figure 5. Dose-dependent apoptosis induction in the A549 cells by **8a** as revealed by flow cytometry. The A549 cells were treated with **8a** (0-100 µM) for 24 h. Twenty thousand cells in each treatment were acquired using a flow cytometer, and the DNA content of the nuclei was registered on a logarithmic scale. The Sub-G1 region (RN1) represents the percentage of cells undergoing apoptosis. The experiments were repeated three times with similar results. All determinations were made in three replicates, and the values are means ± S. E. M. *P<0.001 compared to vehicle control. A representative figure is shown.

Studies have demonstrated that apoptosis induction plays the most vital role in the cancer treatment[37]. Dysregulation in apoptotic pathways has been implicated in the development and progression of malignant tumors as well as occurrence of chemo-resistant phenotypes[38, 39]. In the

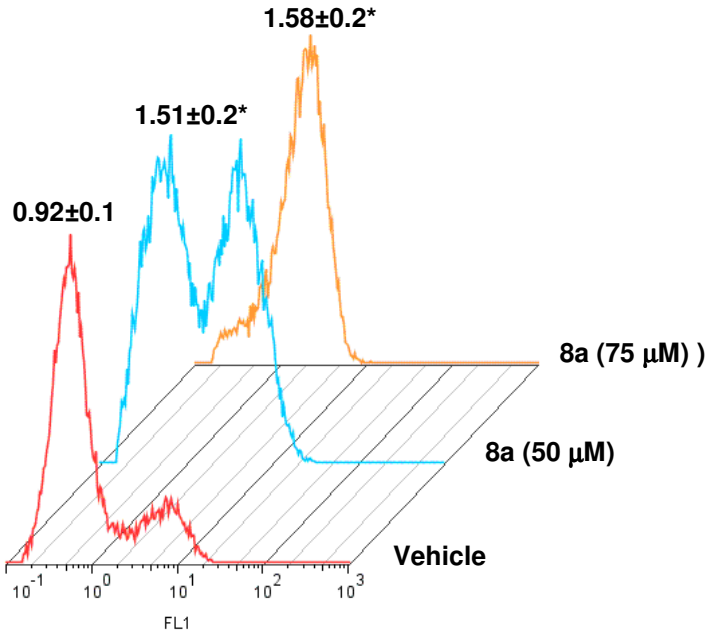

Figure 6. Apoptosis induction in the A549 cells by **8a** as revealed by annexin V/PI assay. The A549 cells (1×10^5 / well) were treated with vehicle (0.1% DMSO) or **8a** (50 or 75 μM) for 8 h. The washed cells in PBS were stained with annexin V and PI, and the annexin positive cells were counted with a fluorescence microscope. A representative figure is shown. The experiments were repeated three times with similar results, all determinations were made in six replicates, and the error bars show the standard errors. **P*<0.01 compared to control.

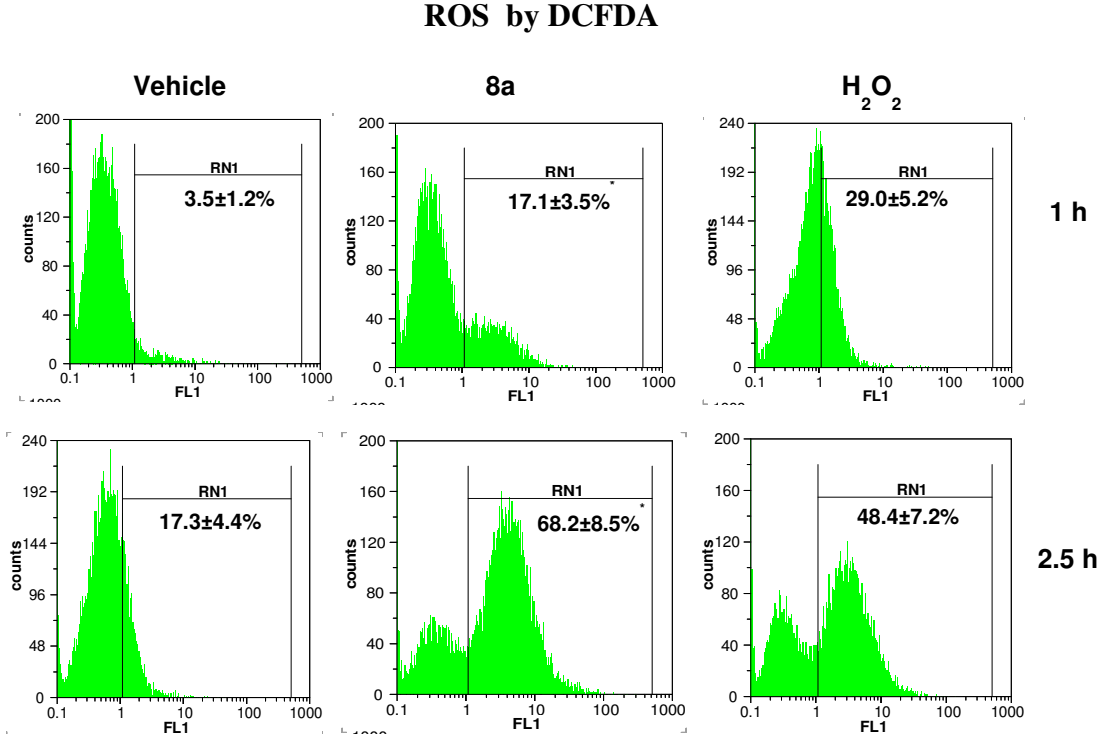

Figure 7. ROS generation in the A549 cells by **8a**. The cells (1 × 105/well), treated with vehicle (0.1% DMSO) or **8a** (75 μM) or H_2O_2 (25 μM) for different times (1 h and 2.5 h) were incubated with DCFH-DA, and the ROS level analyzed by flow cytometry. A representative figure is shown. The experiments were repeated three times with similar results, all determinations were made in six replicates, and the error bars show the standard errors. *P<0.01 compared to control.

present study, apoptosis induction by **8a** was confirmed by quantifying the sub G1 population in the cells, treated with different concentrations (25, 50, 75 and 100 µM) of **8a** at 24 h (Table 1). A dose-dependent increase in the sub-G1 cell population in the flow cytometry revealed induction of apoptosis by **8a**. Compared to control, the increase in the sub-G1 phase cell population ranged from 22-67% when the compound concentration was raised from 50-100 µM (Figure 5). Under the same conditions, the known anti-cancer drug, camptothecin (2 µM) increased the sub-G1 cell population by 36.5±2.4%, compared to control. The annexin V/PI protocol measures the translocation of phosphatidyl serine from the inner to the outer leaflet of the plasma membrane, one of the earliest features of apoptosis. Consistent with the sub-G1 results, treatment of the A549 cells with **8a** increased annexin V positive cells, revealing apoptosis induction. Compared to the mean florescence intensity (MFI) of the vehicle-treated cells was 0.921 that was significantly (P<0.01) increased to 1.51 and 1.58 respectively in the cells, incubated with **8a** (50 and 75 µM) for 8 h (Figure 6).

The reactive oxygen species (ROS) often acts as the signal for apoptosis in many cell types[40]. Hence, the constitutively up-regulated ROS levels, originating from metabolic alterations in malignant cells provides an opportunity for developing selective redox chemotherapeutics[41]. Several anti-cancer agents act via ROS-mediated apoptosis induction. ROS may modulate both anti-apoptotic, and pro-apoptotic effects to restrict tumorigenicity and malignant progression[42, 43]. In the present studies, treatment of the cells with **8a** (75 µM) or the positive control, H_2O_2 (25 µM) increased the ROS generation time-dependently (Figure 7). Compared to the control cells, the ROS increase (29%) by H_2O_2 was more than that (17%) by **8a** at 1 h. However, at 2.5 h **8a** and H_2O_2 increased the ROS level by 68% and 48% respectively. This suggested that ROS is a potential factor in the cytotoxicity of **8a** to the A549 cells.

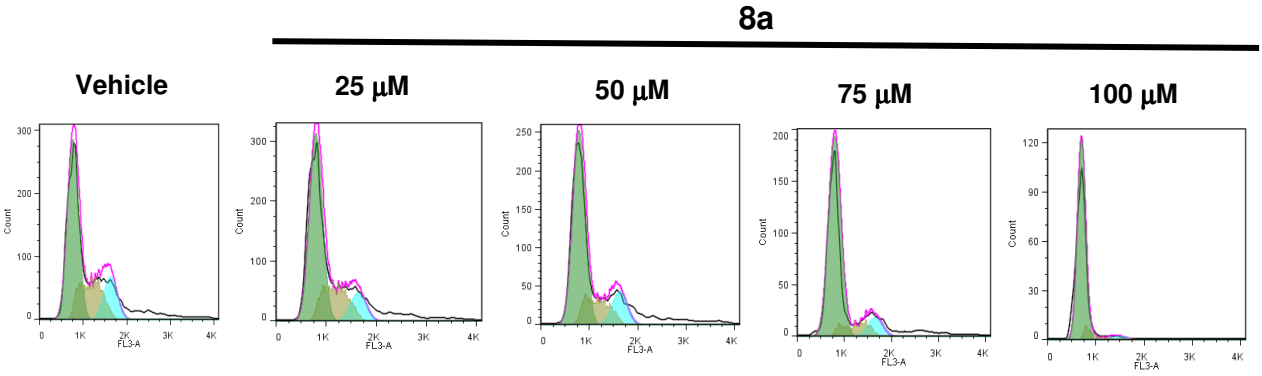

Figure 8. Cell cycle analysis of the A549 cells after treatment with **8a**. The A549 cells were treated with **8a** (0-100 µM) for 24 h. Twenty thousand cells in each treatment were acquired using a flow cytometer, and the DNA content of the nuclei was registered on a linear scale. A representative figure is shown. The experiments were repeated three times with similar results. All determinations were made in three replicates, and the values are means ± S. E. M. *P<0.01 compared to vehicle control.

Inhibition of deregulated cell cycle progression is an effective strategy to halt in cancer progression[44, 45]. Hence we analyzed the possible inhibitory effect of **8a** (25, 50, 75 and 100 µM) on cell cycle progression at 24 h. A dose-dependent G1 arrest was induced by **8a**, the effect being more pronounced ($P < 0.001$) at a dose of ≥75 µM (Figure 8). This was revealed from the increase in the G1 population, associated with the decrease in the percentage of cells in the S-and G2-phases. Taken together, **8a** was found to cause cell death of the A549 cells principally by cell cycle arrest in the G1 phase, which might induce cell apoptosis. However, a detailed molecular mechanism is far from clear and requires further exploration.

3. Experimental Section

3.1. General experimental conditions

The chemicals, used for synthesis were procured from Fluka (Seelze, Germany) and Lancaster (UK). Other reagents were of AR grade. All anhydrous reactions were carried out under an Ar atmosphere, using freshly dried solvents. The IR spectra as thin films were scanned with a Jasco model A-202 FT-IR spectrometer. The ^{1}H NMR (200 MHz) and ^{13}C NMR (50 MHz) spectra were recorded with a Bruker AC-200 spectrometer. The chemicals/biochemicals used for the biological experiments were 3-(4,5-dimethylthiazol-2-yl)-2,5-diphenyltetrazolium bromide (MTT), propidium iodide (PI), N-acetylcysteine (NAC), annexin-V kit (all from Sigma Chemicals, St. Luois, MO), Dulbecco's modified Eagle's medium (DMEM, HiMedia, Mumbai), DCFH-DA (Life Technologies, Carlsbad, CA) and fetal bovine serum (FBS, Gibco Life Technologies, Carlsbad, CA).

3.2. Synthesis

3.2.1. Synthesis of the chalcones (7a-b): To a solution of **5a/5b** (50 mmol) and **6a/6b** (50 mmol) in EtOH (10 mL) was added KOH in EtOH (40%, 100 mL). The resultant yellow solution was heated at 60 °C till completion of the reaction (*cf.* TLC, 8-12 h), the mixture poured into ice-water, carefully acidified with aqueous 6N HCl, and extracted with EtOAc (3 × 50 mL). The combined organic extracts were washed with H_2O (2 × 30 mL), brine (2 × 5 mL), dried (Na_2SO_4), and concentrated in vacuo. The residue was purified by column chromatography (silica gel, 7% EtOAc/hexane) to afford pure **7a/7b**.

3.2.1.1. (E)-1,3-Bis(2-hydroxyphenyl)prop-2-en-1-one (7a): yield: 73%; orange solid; mp 157-158 °C; IR ($CHCl_3$): ν 3329, 3019, 1685, 1630, 1604, 1578, 1488, 1458, 1341, 1304, 1214, 1092, 1066, 1024, 989, 863 cm^{-1}; ^{1}H NMR (200 MHz, $CDCl_3$): δ 5.95 (broad s, 1H, Ar-O*H*), 6.83-7.04 (m, 4H), 7.30-7.33 (m, 1H), 7.45-7.53 (m, 1H), 7.60 (dd, *J* = 7.8, 1.4 Hz, 1H), 7.84 (d, *J* = 15.7 Hz, 1H), 7.93 (dd, *J* = 8.1, 1.5 Hz, 1H), 8.20 (d, *J* = 15.7 Hz, 1H), 12.92 (s, 1H, chelated Ar-O*H*); ^{13}C NMR (50 MHz, CD_3COCD_3): δ 116.7, 118.5, 119.3, 120.3, 120.5, 122.2, 129.8, 130.6, 132.8, 136.7, 141.4, 157.8, 164.0, 194.8; Anal. Calcd. for $C_{15}H_{12}O_3$: C, 74.99; H, 5.03%. Found: C, 75.16; H, 4.73 %.

3.2.1.2. (E)-3-(5-tert-Butyl-2-hydroxyphenyl)-1-(2-hydroxy-5-methylphenyl)prop-2-en-1-one (7b): yield: 75%; orange solid; mp 173-174 °C; IR ($CHCl_3$): ν 3584, 3210, 3019, 2955, 1634, 1586, 1547, 1489, 1414, 1341, 1308, 1287, 1261, 1214, 1176, 1135, 1111, 1030, 985, 943 cm^{-1}; ^{1}H NMR (200 MHz, $CDCl_3$): δ 1.33 (s, 9H), 2.34 (s, 3H), 6.79 (d, *J* = 8.4 Hz, 1H), 6.92 (d, *J* = 8.4 Hz, 1H), 7.29-7.33 (m, 2H), 7.54-7.69 (m, 2H), 7.85 (d, *J* = 15.6 Hz, 1H), 8.1 (d, *J* = 15.6 Hz, 1H), 12.83 (broad s, 1H, chelated Ar-O*H*); ^{13}C NMR (50 MHz, CD_3COCD_3): δ 20.4, 31.7, 34.6, 116.8, 118.7, 120.6, 121.9, 127.1, 128.6, 130.4, 130.6, 138.0, 142.5, 143.4, 156.1, 162.4, 195.2; Anal. Calcd. for $C_{20}H_{22}O_3$: C, 77.39; H, 7.14%. Found: C, 77.54; H, 7.44%.

3.2.2. Synthesis of 1,3-diarylpropanes (8a-b): A suspension of the chalcone **7a** (20 mmol) and 10% Pd-C (0.8 g) in glacial acetic acid (100 mL) was stirred under a slight positive pressure of H_2 at ambient temperature. After completion of the reaction, the mixture was passed through a pad of celite, and the eluate was concentrated in vacuo. The residue was purified by column chromatography (silica gel, 15% EtOAc/hexane) to afford pure **8a.** In a similar way, **8b** was obtained from **7b**.

3.2.2.1. 1,3-Bis(2-hydroxyphenyl)propane (8a)[46]: yield: 84%; light brown solid; mp 95-96 °C; IR ($CHCl_3$): ν 3600, 3398, 3019, 2929, 2859, 1590, 1502, 1489, 1455, 1326, 1215, 1168, 1105, 1043, 930, 876 cm^{-1}; ^{1}H NMR (200 MHz, $CDCl_3$): δ 1.96 (quint, *J* = 7.6 Hz, 2H), 2.68 (t, *J* = 7.6 Hz, 4H), 4.92 (broad s, 2H, Ar-O*H*), 6.76 (d, *J* = 8.0 Hz, 2H), 6.82-6.90 (m, 2H), 7.04-7.16 (m, 4H); ^{13}C NMR (50 MHz, $CDCl_3$): δ 29.7, 30.0, 115.4, 120.7, 127.0, 128.4, 130.1, 153.4; Anal. Calcd. for $C_{15}H_{16}O_2$: C, 78.92; H, 7.06%. Found: C, 79.10; H, 7.11%.

3.2.2.2. 1-(2-Hydroxy-5-methylphenyl)-3-(2-hydroxy-5-tert-butylphenyl)propane (8b): yield: 72%; colorless solid; mp 74-75 °C; IR ($CHCl_3$): ν 3401, 3016, 2962, 2863, 1705, 1610, 1509, 1421, 1268, 1218, 1126, 1111, 818 cm^{-1}; ^1H NMR (200 MHz, $CDCl_3$): δ 1.27 (s, 9H), 1.91-2.05 (m, 2H), 2.25 (s, 3H), 2.60-2.70 (m, 4H), 3.52 (broad s, 2H, Ar-O*H*), 6.68 (t, *J* = 7.6 Hz, 2H), 6.85-6.94 (m, 2H), 7.06-7.14 (m, 2H); ^{13}C NMR (50 MHz, $CDCl_3$): δ 20.3, 29.9, 30.3, 30.4, 31.4, 33.8, 115.2, 115.5, 123.7, 127.1, 127.4, 127.8, 128.3, 129.8, 130.8, 143.4, 150.8, 150.9; Anal. Calcd. for $C_{20}H_{26}O_2$: C, 80.50; H, 8.78%. Found: C, 80.16; H, 8.61%.

3.2.3. 1,3-Bis(5-bromo-2-hydroxyphenyl)propane (9): A solution of **8a** (0.46 g, 2.0 mmol) and $CuBr_2$ (1.88 g, 8.4 mmol) in dry MeCN (10 mL) was stirred at ambient temperature till the completion of the reaction (*cf*. TLC, 8 h). The reaction mixture was concentrated in vacuo, H_2O (20 mL) was added to the mixture, extracted with EtOAc (2 x 10 mL), and the extract was passed through a pad of celite. The celite bed was washed with EtOAc (2 × 5 mL) and the organic extract washed with H_2O (2 × 10 mL) brine (5 mL), and dried (Na_2SO_4). Removal of the solvent in vacuo followed by purification by column chromatography (silica gel, 15% EtOAc/ hexane) of the residue afforded pure **9**. yield: 98%; colorless solid; mp 132-133 °C; IR ($CHCl_3$): ν 3602, 3233, 3019, 2927, 2859, 1492, 1455, 1428, 1321, 1214, 1171, 1123 cm^{-1}; ^1H NMR (200 MHz, $CDCl_3$): δ 1.90 (quint, *J* = 7.5 Hz, 2H), 2.62 (t, *J* = 7.5 Hz, 4H), 4.92 (broad s, 2H, Ar-O*H*), 6.63 (d, *J* = 8.4 Hz, 2H), 7.16 (dd, *J* = 8.4, 2.5 Hz, 2H), 7.23-7.24 (m, 2H); ^{13}C NMR (50 MHz, $CDCl_3$): δ 29.2, 29.5, 112.8, 117.0, 129.9, 130.5, 132.8, 152.6; Anal. Calcd. for $C_{15}H_{14}Br_2O_2$: C, 46.66; H, 3.65; Found: C, 47.04; H, 3.65%.

3.2.4. Formylation of 9: To a stirred solution of **9** (3.89 g, 10 mmol), Et_3N (7.80 mL, 56 mmol), and anhydrous $MgCl_2$ (5.90 g, 62 mmol) in dry MeCN (100 mL) was added paraformaldehyde (2.16 g, 72 mmol) in portions. The mixture was refluxed for 8 h, cooled to room temperature, acidified with aqueous 3N HCl, and extracted with Et_2O (3 × 15 mL). The ether layer was washed with H_2O (2 × 10 mL), brine (5 mL), and dried (Na_2SO_4). Removal of the solvent in vacuo followed by purification by column chromatography (silica gel, 10% EtOAc/ hexane) of the residue afforded pure **10** and **11**.

3.2.4.1. 1-(5-Bromo-3-formyl-2-hydroxyphenyl)-3-(5-bromo-2-hydroxyphenyl)propane (10): yield: 33%; colorless solid; mp 135-136 °C; IR ($CHCl_3$): ν 3584, 3325, 3019, 2922, 2859, 1714, 1658, 1608, 1493, 1446, 1269, 1214, 1042 cm^{-1}; ^1H NMR (200 MHz, $CDCl_3$): δ 1.87-1.95 (m, 2H), 2.59-2.73 (m, 4H), 4.94 (broad s, 1H, Ar-O*H*), 6.62 (d, *J* = 8.4 Hz, 1H), 7.13-7.18 (m, 1H), 7.22 (m, 1H), 7.48-7.51 (m, 2H), 9.80 (s, 1H), 11.23 (s, 1H, chelated Ar-O*H*); ^{13}C NMR (50 MHz, $CDCl_3$): δ 28.7, 29.2, 29.8, 111.1, 111.3, 117.2, 122.0, 129.9, 131.5, 132.8, 134.0, 134.1, 139.5, 154.8, 158.9, 197.4; Anal. Calcd. for $C_{16}H_{14}Br_2O_3$: C, 46.41; H, 3.41; Found: C, 46.63; H, 3.65%.

3.2.4.2. 1,3-Bis(5-bromo-3-formyl-2-hydroxyphenyl)propane (11): yield: 47%; colorless solid; mp 156-157 °C; IR ($CHCl_3$): ν 3390, 3019, 2932, 2842, 1731, 1658, 1606, 1437, 1263, 1214, 1047, 998 cm^{-1}; ^1H NMR (200 MHz, CD_3COCD_3): δ 1.97 (quint, *J* = 7.7 Hz, 2H), 2.74 (t, *J* = 7.7 Hz, 4H), 7.64 (d, *J* = 2.4 Hz, 2H), 7.80 (d, *J* = 2.4 Hz, 2H), 9.97 (s, 2H), 11.36 (s, 2H, chelated Ar-O*H*); ^{13}C NMR (50 MHz, CD_3COCD_3): δ 30.4, 31.3, 111.3, 122.4, 134.0, 134.5, 139.8, 159.2, 197.8; Anal. Calcd. for $C_{17}H_{14}Br_2O_4$: C, 46.18; H, 3.19; Found: C, 46.32; H, 3.22%.

3.2.5. 1,3-Bis(5-bromo-2-hydroxy-3-hydroxymethylphenyl)propane (12): To an ice-cooled solution of **11** (0.88 g, 2 mmol) in dry MeOH (10 mL) was added $NaBH_4$ (0.08 g, 2 mmol) and the mixture and stirred at 0 °C till complete consumption of **11** (*cf*. TLC, 3 h). The reaction was quenched with aqueous saturated NH_4Cl solution (5 mL) and concentrated in vacuo. The residue was extracted with EtOAc (3 × 10 mL), the organic extract washed with H_2O (2 × 10 mL) and brine (5 mL), and dried (Na_2SO_4). Removal of the solvent in vacuo followed by purification by column chromatography (silica gel, 30% EtOAc/hexane) of the residue afforded pure **12**. yield: 71%; colorless solid; mp 174-175 °C; IR ($CHCl_3$): ν 3395, 3297, 3019, 2927, 2854, 1468, 1451, 1427, 1353, 1214, 1020 cm^{-1}; ^1H NMR (200 MHz, CD_3COCD_3): δ 1.89 (quint, *J* = 7.7 Hz, 2H), 2.67 (t, *J* = 7.7 Hz, 4H), 4.80 (d, *J* = 4.8 Hz, 4H), 5.14 (t, *J* = 4.8 Hz, 2H, CH_2-O*H*), 7.12 (d, *J* = 2.5 Hz, 2H), 7.20 (d, *J* = 2.5 Hz, 2H), 8.45 (s, 2H, Ar-

O*H*); ^{13}C NMR (50 MHz, CD_3COCD_3): δ 29.5, 30.0, 62.4, 110.9, 127.7, 128.5, 131.2, 131.9, 153.4; Anal. Calcd. for $C_{17}H_{18}Br_2O_4$: C, 45.77; H, 4.07; Found: C, 45.90; H, 3.96%.

3.3. Biological assays

3.3.1. Cell culture

The A549 cell line, procured from National Centre for Cell Science, Pune, India were cultured in DMEM medium, supplemented with 10% FBS, 100 U/mL penicillin and 100 µg/mL streptomycin. The cells were grown at 37 °C under an atmosphere of 5% CO_2.

3.3.2. MTT assay

Viabilities of the control cells and those treated with various concentrations of the test compounds were determined at 48 h by the MTT reduction assay[47]. Briefly, cells (1×10^4/well) grown in 96-well plates were incubated overnight at 37 °C under an atmosphere of 5% CO_2. Next day the cells were incubated with vehicle (0.1% DMSO) or various concentrations of the test compounds for 48 h. The cells were washed once with PBS, MTT solution (0.5 mg/mL, 100 µL) was added to each well and kept at 37 °C for 6 h. The formazan crystals in the viable cells were solubilized with 0.01 N HCl (100 µL) containing 10% SDS and the absorbance at 550 nm.

3.3.3. Cell morphology study

The A549 cells (1×10^5 /well) in 6-well plates were incubated with vehicle (0.1% DMSO) or the test compounds for 24 h. The cells were washed twice with PBS and seen under a phase contrast microscope. Representative fields of the cells were photographed using an Axioskop II Mot plus (Zeiss) microscope.

3.3.4. Fluorescence microscopy

DNA double staining was used to differentiate between apoptotic and necrotic cells. Cells were treated with different compounds for 3 h, and subsequently stained with Hoechst 33342 (20 mM) and PI (50 mg/mL) for 15 min. Cells were washed, mounted with 70% glycerol, and analyzed under an Axioskop II Mot plus (Zeiss) microscope (40 × optics).

3.3.5. Flow cytometry

We analyzed hypodiploid DNA content as a marker for apoptosis by flow cytometry, after staining with PI. The cells incubated with **8a** (0-100 µM) for 24 h were washed with cold PBS and fixed in 70% chilled ethanol. Further, the cells were washed two times with cold PBS, incubated with PI (400 µg/mL) and RNAse A (200 µg/mL) in 1 mL hypotonic buffer (0.1% sodium citrate and 0.1% Triton X-100) for 30 min at 37 °C, and analyzed with a Pertec CyFlow® Space flow cytometer using the FlowJo program. Cellular debris was excluded from the analyses by raising the forward scatter threshold, and the DNA content of the nuclei was registered on a logarithmic scale. At least 2×10^4 cells of each sample were analyzed. The apoptotic nuclei appeared as broad hypodiploid DNA peaks. For cell cycle analysis, the DNA content of the nuclei was registered on a linear scale.

3.3.6. Annexin V assay

The PS translocation in the A549 cells was detected using an annexin V apoptosis detection kit as per the manufacturer's instructions. Briefly, the untreated and **8a** (50 and 75 µM)-treated cells (1×10^5/well) were incubated for 8 h, the cells were washed two times with cold PBS, resuspended in a binding buffer (1 mL) and stained with annexin V (5 µL). After incubating for 15 min at room temperature in the dark, the annexin V-positive cells were counted using a Pertek FAC Scan flow

cytometer. The increase in the mean fluorescence intensity (MFI) reflected the annexin V positive cells.

3.3.7. ROS assay

The ROS levels in the cells were estimated from the ROS-mediated fluorescence enhancement of the cell permeable oxidation sensitive probe, DCFH-DA[48]. The cells (1×10^5/well), treated with **8a** (75 μM) for 1 h and 2.5 h were scraped, centrifuged at 750 × g, and washed three times with PBS. After incubating with DCFH-DA (final concentration 5 μM) in PBS for 20 min at 37 °C, the cells were washed three times with cold PBS and analyzed using a Pertek FACScan flow cytometer. H_2O_2 (25 μM) was used as the positive control.

4. Conclusion

Overall, our present findings showed pronounced cytotoxicity of six synthesized diarylpropanes, against the human lung cancer A549 cells. However, the activity of the brominated diarylpropanes (**9-12**) was primarily via necrosis. Nevertheless consistent with the previous report, our results also established the importance of OH groups at the phenyl rings in the anti-cancer property of the test compounds. Previously none of the naturally occurring diarylpropanes exhibited any toxicity to the lung cancer NCI-H187 cells, although some of them were very effective against human epidermoid carcinoma (KB) cells[20]. Interestingly, our results established that **8a** can induce apoptosis to the A549 cells that was mechanistically rationalized in terms of cell cycle arrest and ROS generation. The activity of **8a** was also compared with an anti-cancer drug camptothecin. The positive outcome of the in vitro study could form a strong basis for the development of some diarylpropanes as novel agents for human lung cancer prevention and/or intervention. However, this warrants further in vitro evaluation of other analogues of **8a** to potentiate the activity so that these can be used for in vivo studies at pharmacologically achievable doses. In this regard, appropriate substitutions at the phenyl rings might arrange the aryl groups at a desired dihedral angle between them to improve their binding with tubuline such as phenstatin, combretastatin, and podophylotoxin. This might reduce their MIC for inhibiting the cancer cell proliferation.

References

[1] Korkina, L. G. Phenylpropanoids as naturally occurring antioxidants: from plant defense to human health. *Cell Mol. Biol*. **2007**, *53*, 15–25.
[2] Hemaiswarya, S.; Doble, M. Synergistic interaction of phenylpropanoids with antibiotics against bacteria. *J. Med. Microbiol*. **2010**, *59*, 1469–1476.
[3] Ito, C.; Itoigawa, M.; Furukawa, H.; Ichiishi, E.; Mukainaka, T.; Okuda, M.; Ogata, M.; Tokuda, H.; Nishino, H. Anti-tumor-promoting effects of phenylpropanoids on Epstein-Barr virus activation and two-stage mouse skin carcinogenesis. *Cancer Lett*. **1999**, *142*, 49–54.
[4] Itoigawa, M.; Ito, C.; Tokuda, H.; Enjo, F.; Nishino, H.; Furukawa, H. Cancer chemopreventive activity of phenylpropanoids and phytoquinoids from Illicium plants. *Cancer Lett*. **2004**, *214*, 165–169.
[5] Hemaiswarya, S.; Doble, M. Combination of phenylpropanoids with 5-fluorouracil as anti-cancer agents against human cervical cancer (HeLa) cell line. *Phytomedicine* **2013**, *20*, 151–158.
[6] Ni, L.; Meng, Q. M.; Siroski, J. A. Recent advances in therapeutic chalcones. *Expert Opin. Ther. Pat*. **2004**, *14*, 1669–1691.
[7] Majumdar, I. D.; Devanabanda, A.; Fox, B.; Schwartzman, J.; Cong, H.; Porco Jr., J. A.; Weber, H. C. Synthetic cyclohexenyl chalcone natural products possess cytotoxic activities against prostate cancer cells and inhibit cysteine cathepsins in vitro. *Biochem. Biophys. Res. Commun*. **2011**, *416*, 397–402.
[8] Palermo, C.; Joye, J. A. Cysteine cathepsin proteases as pharmacological targets in cancer. *Trends Pharmacol. Sci*. **2008**, *29*, 22–28.
[9] Adjei, A. A.; Rowinsky, E. K. Novel anticancer agents in clinical development. *Cancer Biol. Ther*. **2003**, *2*, S5–S15.
[10] Neidle, S.; Thurston, D. E. Chemical approaches to the discovery and development of cancer therapies. *Nat. Rev. Cancer* **2005**, *5*, 285–296.

[11] Kamb, A.; Wee, S.; Lengauer, C. Why is cancer drug discovery so difficult? *Nat. Rev. Drug Discov*. **2007**, *6*, 115–120.
[12] Pujol, M. D.; Romero, M.; Sanchez, I. Synthesis and biological activity of new class of dioxygenated anticancer agents. *Curr. Med. Chem. Anticancer Agents* **2005**, *5*, 215–237.
[13] Gribble, G. W. The diversity of naturally produced organohalogens. *Chemosphere* **2003**, *52*, 289–297.
[14] Laatsch, H.; Renneberg, B.; Hanefeld, U.; Kellner, M.; Pudleiner, H.; Hamprecht, G.; Kraemer, H. P.; Anke, H. Structure-activity relationships of phenyl and benzoylpyrroles. *Chem. Pharm. Bull.* **1995**, *43*, 537–546.
[15] Gribble, G. W. Naturally occurring organohalogen compounds. *Acc. Chem. Res.* **1998**, *31*, 141–152.
[16] Segraves, E. N.; Sui, J. K.; Shah, R. R.; Kenyon, V. A.; Segraves, N. L.; Cichewicz, R. H.; Johnson, T. A.; Crews, P.; Whitman, S.; Holman, T. R. Probing the activity differences of simple and complex brominated aryl compounds against 15-Soybean, 15-Human, and 12-Human Lipoxygenase. *J. Med. Chem.* **2004,** *47,* 4060–4065.
[17] Sweety, Kumar, S.; Nepali, K.; Sapra, S.; Suri, O. P.; Dhar, K. L.; Sarma, G. S.; Saxena, A. K. Synthesis and biological evaluation of chalcones having heterosubstituent(s). *Ind. J Pharm Sci*. **2010**, *72*, 801–806.
[18] Kim, S. -H.; Lee, E.; Baek, K. H.; Kwon, H. B.; Woo, H.; Kwon, Y.; Na, Y. Chalcones, inhibitors for topoisomerase I and cathepsin B and L, as potential anti-cancer agents. *Bioorg. Med. Chem. Lett*. **2013**, *23*, 3320–3324.
[19] Boyer, N.; Morrison, K. C.; Kim, J.; Hergenrother, P. J.; Movassaghi, M. Synthesis and anticancer activity of epipolythiodiketopiperazine alkaloids. *Chem. Sci.* **2013**, *4*, 1646–1657.
[20] Moosophon, P.; Kanokmedhakul, S.; Kanokmedhakul, K. Diarylpropanes and an arylpropyl quinone from *Combretum griffithii. J. Nat. Prod*. **2011**, *74*, 2216–2218.
[21] Smitinand, T. Thai Plant Names. Revised edition. Prachachon Co., Ltd.: Bangkok, **2001**; pp 145–146.
[22] Pathommapas, N.; Prajudthasri, N.; Wongsa, N.; Homsombat, P.; Sritubtim, S. The Thai local wisdom of medicinal plants usage from Phu Dong Ee-Pia forest, Ubonratana district, Khon Kaen province. *UDRU J. Sci. Technol. Centre* **2008**, *6*, 59–87.
[23] Guha, P.; Dey, A.; Sarkar, B.; Dhyani, M. V.; Chattopadhyay, S.; Bandyopadhyay, S. K. Improved antiulcer and anticancer properties of a trans-resveratrol analog in mice. *J. Exp. Pharmacol. Ther*. **2009**, *328*, 829-838.
[24] Patro, B. S.; Maity, B.; Chattopadhyay, S. Topoisomerase inhibitor coralyne photosensitizes DNA, leading to elicitation of Chk2-dependent S-phase checkpoint and p53-independent apoptosis in cancer cells. *Antiox. Redox. Signal*. **2010**, *12*, 945–960.
[25] Guha, P.; Dey, A.; Chatterjee, A.; Chattopadhyay, S.; Bandyopadhyay, S. K. Pro-ulcer effects of resveratrol in mice with indomethacin-induced gastric ulcers are reversed by l-arginine. *Brit. J. Pharmacol*. **2010**, *159*, 726–734.
[26] Patro, B. S.; Tyagi, M.; Saha, J.; Chattopadhyay, S. Comparative nuclease and anti-cancer properties of the naturally occurring malabaricones. *Bioorg. Med. Chem*. **2010**, *18*, 7043–7051.
[27] Guha, P.; Dey, A.; Sen, R.; Chatterjee, M.; Chattopadhyay, S.; Bandyopadhyay, S. K. Calpain and caspase orchestrated death signal to accomplish apoptosis induced by resveratrol and its novel analog hydroxstilbene-1 in cancer cells. *J. Pharmacol. Exp. Ther.* **2010**, *334*, 381–394.
[28] Guha, P.; Dey, A.; Sen, R.; Chatterjee, M.; Chattopadhyay, S.; Bandyopadhyay, S. K. Intracellular GSH depletion triggered mitochondrial bax translocation to accomplish resveratrol-induced apoptosis in the U937 cell line. *J. Pharmacol. Exp. Ther.* **2011**, *336*, 206–214.
[29] Mohanty, J.; Pal, H.; Nayak, S. K.; Chattopadhyay, S.; Sapre, A. V. Excited singlet (S_1) state interactions of calixarenes with chloroalkanes: A combination of concerted and stepwise dissociative electron transfer mechanism. *J. Chem. Phys*. **2002**, *117*, 10744–10751.
[30] Semwal, A.; Bhattacharya, A.; Nayak, S. K. Ultrasound mediated selective monoalkylation of 4-*tert*-butyl-calix[6]arene at the lower rim. *Tetrahedron* **2002**, *58*, 5287–5290.
[31] Bhattacharya, S.; Nayak, S. K.; Semwal, A.; Chattopadhyay, S.; Banerjee, M. Study of host−guest interaction of [70] fullerene with substituted calix[6]arenes by absorption spectrometric method. *J. Phys. Chem. A* **2004**, *108*, 9064–9068.
[32] Bhatt, S.; Nayak, S. K. Reductive deoxygenation of ortho-hydroxyaromatic aldehydes to 1,2-bis(hydroxyaryl)ethanes: application to the synthesis of ethylene bridged calixarene-analogous metacyclophanes. *Tetrahedron Lett*. **2009**, *50*, 5823–5826.
[33] Bhatt, S.; Nayak, S. K. Copper(II)bromide: a simple and selective monobromination reagent for electron-rich aromatic compounds. *Synth. Commun*. **2007**, *37*, 1381–1388.
[34] Hansen, T. V.; Skattebøl, L. *ortho*-Formylation of phenols; preparation of 3-bromosalicylaldehyde. *Org. Synth.* **2005**, *82*, 64–68.

[35] Slatore, C. G.; Gould, M. K.; Au, D. H.; Deffebach, M. E.; White, E. Lung cancer stage at diagnosis: individual associations in the prospective VITamins and lifestyle (VITAL) cohort. *BMC Cancer* **2011**, *11*, 228 doi:10.1186/1471-2407-11-228.
[36] Indran, I. R.; Tufo, G.; Pervaiz, S.; Brenner, C. Recent advances in apoptosis, mitochondria and drug resistance in cancer cells. *BBA – Bioener*. **2011**, *6*, 735–745.
[37] Evan, G. I.; Vousden, K. H. Proliferation, cell cycle and apoptosis in cancer. *Nature* **2001**, *411*, 342–343.
[38] Arends, M. J.; Wyllie, A. H. Apoptosis: mechanisms and roles in pathology. *Int. Rev. Exp. Pathol*. **1991**, *32*, 223–254.
[39] Hickman, J. A. Apoptosis and chemotherapy resistance. *Eur. J. Cancer* **1996**, *32*, 921–926.
[40] Buttke, T. M.; Sandstrom, P. A. Oxidative stress as a mediator of apoptosis. *Immunol. Today* **1994**, *15*, 7–10.
[41] Wondrak, G. T. Redox-directed cancer therapeutics: molecular mechanisms and opportunities. *Antiox. Redox Signal*. **2009**, *11*, 3013–3069.
[42] Cabello, C. M.; Bair, W. B.; Wondrak, G. T. Experimental therapeutics: targeting the redox Achilles heel of cancer. *Curr. Opin. Investig. Drugs* **2007**, *8*, 1022–1037.
[43] Fruehauf, J. P.; Meyskens Jr., F. L. Reactive oxygen species: a breath of life or death? *Clin. Cancer Res*. **2007**, *13*, 789–794.
[44] Grana, X.; Reddy, E. P. Cell cycle control in mammalian cells: role of cyclins, cyclin dependent kinases (CDKs), growth suppressor genes and cyclin-dependent kinase inhibitors (CKIs). *Oncogene* **1995**, *11*, 211–219.
[45] Singh, R.P.; Dhanalakshmi, S.; Agarwal, R. Phytochemicals as cell cycle modulators a less toxic approach in halting human cancers. *Cell Cycle* **2002**, *1*, 156–161.
[46] Halligudi, S. B.; Sajanikumari, C. S.; Kala Raj, N. K.; Deshpande, S. S; Degaonkar, M. P. Liquid phase allylation of phenol using Hβ zeolite. *J. Mol. Catal. A: Chem*. **2001**, *175*, 161-167.
[47] Mosmann, T. Rapid colorimetric assay for cellular growth and survival: application to proliferation and cytotoxicity assays. *J. Immunol. Meth*. **1983**, *65*, 55–63.
[48] Balasubramanyam, K.; Altaf, M.; Varier, R. A.; Swaminathan, V.; Ravindran, A.; Sadhale, P. P.; Kundu, T. K. Polyisoprenylated benzophenone, garcinol, a natural histone acetyltransferase inhibitor, represses chromatin transcription and alters global gene expression. *J. Biol. Chem*. **2004**, *279*, 33716–33726.